Stability of Poiseuille flow in a fluid overlying an anisotropic and inhomogeneous porous layer

P. Deepu,[1] Prateek Anand,[2] and Saptarshi Basu[2]
[1]*Department of Mechanical and Aerospace Engineering, University of Florida, Gainesville, Florida 32611, USA*
[2]*Indian Institute of Science, Bangalore 560012, India*
(Received 15 April 2015; published 6 August 2015)

We present the linear stability analysis of horizontal Poiseuille flow in a fluid overlying a porous medium with anisotropic and inhomogeneous permeability. The generalized Darcy model is used to describe the flow in the porous medium with the Beavers-Joseph condition at the interface of the two layers and the eigenvalue problem is solved numerically. The effect of major system parameters on the stability characteristics is addressed in detail. It is shown that the anisotropic and inhomogeneous modulation of the permeability of the underlying porous layer provides an effective means for passive control of the flow stability.

DOI: 10.1103/PhysRevE.92.023009 PACS number(s): 47.15.Rq, 47.15.Fe, 47.56.+r

I. INTRODUCTION

Flow through a porous-fluid double layer is encountered in numerous geophysical and engineering systems such as deep filtrations, separation processes, biological tissues, chemical and nuclear reactors, oil recovery, electronics cooling, heat pipes, and boiling, to name a few. While thermal convection related instabilities in such systems have been extensively studied [1,2], pure hydrodynamic instabilities in such flows have received attention in the literature only in recent years. In particular, we are interested in plane Poiseuille flow in superposed fluid-porous layers in isothermal conditions. Chang *et al.* [3] were the first to consider such a problem, where the linear stability of Poiseuille flow in a Newtonian fluid overlying a porous layer was studied. By numerically solving the Navier-Stokes–Darcy model, they identified three distinct modes of instability, each of which manifests itself as a minimum in the neutral stability curve. The minimum of the curve in the low wave number region corresponds to the porous-layer mode (referred to hereafter as PM), where the porous medium controls the system stability. In the short-wave mode (or the right-hand lobe in the curve), most of the flow perturbations are confined in the fluid layer and the corresponding perturbed stream function is antisymmetric about the center line of the fluid layer. Hence this mode is termed as the odd-fluid layer mode (OFM). The instability mode that appears in the moderate wave number region exhibits even symmetry with respect to the center line of the fluid and is essentially a pure fluid layer mode, referred to as the even-fluid layer mode (EFM). EFM is not present in the thermal convection problem of the superposed fluid-porous layer [2], where the basic state is quiescent, and can be deemed as the equivalent of even-shear mode in single-layer Poiseuille flow. Depending upon the values of the different physical parameters, any of these modes can dominate the stability of the system. For example, at very high values of depth ratio (ratio of thickness of the fluid layer to that of the porous layer), the flow through the double-layer system behaves similarly to a Poiseuille flow with a porous-slip bottom wall and hence EFM is likely to dominate. On the other hand, at very low depth ratios, most of the perturbed flow occurs in the porous layer and hence PM is likely to dominate.

Liu *et al.* [4] investigated the same problem using the Brinkman model and showed that OFM does not appear for the same conditions as in Chang *et al.* [3], since the continuity of velocity at the porous-fluid interface leads to an even symmetry of the basic and perturbed states. Hence the odd-fluid disturbances are precluded. More detailed models for the problem have also been developed; for instance, Hill and Straughan [5] employed a three-layered approach, where a Brinkman porous layer is introduced between the fluid and Darcian-porous layers. Silin *et al.* [6] examined this problem experimentally to validate the results of linear stability analysis. The inherent assumption in all these studies is that the permeability of the porous medium is isotropic and homogeneous. But in practical situations, the permeability of a porous layer can have directional and/or spatial variations [7–9]. Hence in this paper, we intend to address the effects of anisotropy and inhomogeneity in the permeability of the porous medium on the stability of plane Poiseuille flow of a Newtonian fluid overlying and saturating the porous layer.

Recently, Deepu *et al.* [10] has investigated similar effects on the stability of free surface flow in an inclined superposed fluid-porous layer system. However, the stability characteristics of the present system are starkly different, predominantly due to the changes in the problem formulation and boundary conditions. With the presence of a free interface, the two major instability modes present in the gravity-driven problem are the long-wave surface mode and the shear mode [11,12], as opposed to the shear-driven modes of instability in the present problem. The change in the problem definition reflects in the parametric domain as well; for example, both the surface and shear modes depend on the surface tension of the fluid and angle of inclination [13], while these parameters do not appear in the present problem of horizontal channel flow. In Deepu *et al.* [10], we showed that the surface mode is a pure fluid mode and hence is insensitive to the anisotropic and inhomogeneous changes in the permeability of the underlying porous layer. In contrast, for the present case of Poiseuille flow, the fluid modes are also found to be very sensitive to such effects. In addition, in the former problem, the surface mode is always observed to be the critical instability mode, but here we report a fascinating dominance switching phenomenon among the different modes under certain conditions. Noting the fundamental differences between the two problems, the present study aims to report findings on the stability dynamics of internal flow in the context of superposed fluid-porous layers and caters to benefit applications that specifically employ similar flows (such as

oil recovery, deep filtration, and thermocline-based energy storages). The question as to which model describes the flow in a porous medium most accurately is still open [4]. In the present study, to keep the analysis simple, we elect to use Darcy's law and derive the perturbation equations for the current problem and solve the eigenvalue problem using the Chebyshev collocation method. In the parametric range considered, our results show that the stability of the system drastically changes when the anisotropic and inhomogeneous effects are included.

II. FORMULATION OF THE PROBLEM

Let us consider a superposed horizontal porous layer of thickness d_m underlying a fluid layer of thickness d. A Cartesian coordinate system with x in the mean flow direction and z in the vertical direction measured from the fluid-porous interface is chosen. The continuity and momentum equations for the fluid layer are [3]

$$\frac{\partial u}{\partial x}+\frac{\partial w}{\partial z}=0, \tag{2.1}$$

$$\frac{\partial u}{\partial t}+u\frac{\partial u}{\partial x}+w\frac{\partial u}{\partial z}=-\frac{1}{\rho}\frac{\partial p}{\partial x}+\nu\Delta u, \tag{2.2}$$

$$\frac{\partial w}{\partial t}+u\frac{\partial w}{\partial x}+w\frac{\partial w}{\partial z}=-\frac{1}{\rho}\frac{\partial p}{\partial z}+\nu\Delta w, \tag{2.3}$$

where u and w are the x and z components of the fluid velocity, p is the pressure, ν denotes the kinematic viscosity, and Δ is the two-dimensional Laplace operator.

The corresponding equations for the porous medium are

$$\frac{\partial u_m}{\partial x}+\frac{\partial w_m}{\partial z}=0, \tag{2.4}$$

$$\frac{1}{\phi}\frac{\partial u_m}{\partial t}=-\frac{1}{\rho}\frac{\partial p_m}{\partial x}-\frac{\nu}{K_x\eta_x(z/d_m)}u_m, \tag{2.5}$$

$$\frac{1}{\phi}\frac{\partial w_m}{\partial t}=-\frac{1}{\rho}\frac{\partial p_m}{\partial z}-\frac{\nu}{K_z\eta_z(z/d_m)}w_m, \tag{2.6}$$

where the subscript m denotes the pore-averaged quantities, ϕ is the porosity, and K_x and K_z are the permeabilities in the x and z directions, respectively. η_x and η_z denote the respective inhomogeneity functions. Let us define the anisotropy parameter, $\xi=K_x/K_z$. The above governing equations are the same as that of Chang *et al.* [3], except that the flow model for the porous medium considered here allows the permeability to be anisotropic and inhomogeneous. Note, however, that the inhomogeneity variations could occur both in both the x and z directions. But such a general formulation would lead to a base state that is two dimensional in nature, thus rendering the problem very complicated. Hence, to keep in line with the fully developed base solution considered for the fluid layer (as shown below), the inhomogeneity functions are assumed to be functions of z only.

The boundary conditions are specified as follows. At the bottom of the porous layer, $z=-d_m$, $w_m=0$. The upper boundary is assumed to be a rigid wall; hence at $z=d$, $u=w=0$. At the fluid-porous interface ($z=0$), we employ the Beavers-Joseph condition [14]:

$$\frac{\partial u}{\partial z}=\frac{\alpha_{BJ}}{\sqrt{K_x\eta_x(0)}}(u-u_m), \tag{2.7}$$

where α_{BJ} is the Beavers-Joseph coefficient. Note that the streamwise component of permeability at the interface is used in the above condition [15]. The other two conditions at the interface are the continuity of normal velocity and pressure: $w=w_m$ and $p=p_m$.

Assuming a constant pressure gradient in the x direction, the steady fully developed solution of the base state is given by

$$\begin{aligned}\overline{u}(z)&=\frac{A_1}{2}z^2+A_2z+A_3,\quad \overline{w}=0,\quad 0\leqslant z\leqslant d,\\ \overline{u}_m(z)&=-A_1K_x\eta_x(z),\quad \overline{w}_m=0,\quad -d_m\leqslant z\leqslant 0,\end{aligned} \tag{2.8}$$

where,

$$\begin{aligned}A_1&=\frac{1}{\mu}\frac{\partial p}{\partial x},\quad A_2=\frac{A_1\alpha_{BJ}}{2}\frac{\left[2K_x\eta_x(0)-d^2\right]}{\sqrt{K_x\eta_x(0)}+d\alpha_{BJ}},\\ A_3&=-\frac{A_1d}{2}\frac{[d\sqrt{K_x\eta_x(0)}+2\alpha_{BJ}K_x\eta_x(0)]}{\sqrt{K_x\eta_x(0)}+d\alpha_{BJ}},\end{aligned} \tag{2.9}$$

with μ denoting the dynamic viscosity of the fluid. Normalizing the length scale in the fluid layer by d, that of the porous layer by d_m, and the velocities in both the layers by V, the maximum of $\bar{u}(z)$, we obtain the following nondimensional velocity profile:

$$\begin{aligned}\bar{U}(z)&=C_1z^2+C_2z+C_3,\quad 0\leqslant z\leqslant 1,\\ \bar{U}_m(z_m)&=\frac{8\delta^2}{F}\eta_x(z_m),\quad -1\leqslant z_m\leqslant 0,\end{aligned} \tag{2.10}$$

where

$$\begin{aligned}C_1&=\frac{-4\hat{d}^2}{F},\quad C_2=\frac{4\hat{d}^2\alpha_{BJ}[\hat{d}^2-2\delta^2\eta_x(0)]}{F[\delta\sqrt{\eta_x(0)}+\hat{d}\alpha_{BJ}]},\\ C_3&=\frac{4\hat{d}\delta[2\alpha_{BJ}\delta\eta_x(0)+\hat{d}\sqrt{\eta_x(0)}]}{F[\delta\sqrt{\eta_x(0)}+\hat{d}\alpha_{BJ}]},\\ F&=\frac{\alpha^2{}_{BJ}[\hat{d}^2-2\delta^2\eta_x(0)]^2}{[\delta\sqrt{\eta_x(0)}+\hat{d}\alpha_{BJ}]^2}+\frac{4\hat{d}\delta[2\alpha_{BJ}\delta\eta_x(0)+\hat{d}\sqrt{\eta_x(0)}]}{[\delta\sqrt{\eta_x(0)}+\hat{d}\alpha_{BJ}]}.\end{aligned} \tag{2.11}$$

Here δ is the Darcy number defined as $\sqrt{K_x}/d_m$ and $\hat{d}$ is the depth ratio d/d_m.

By superposing infinitesimal disturbances to the basic state, we now obtain the equations governing the linear stability of the system. The variables are nondimensionalized using d, V, d/V, and $\mu V/d$ as the respective scales of length, velocity, time, and pressure in the fluid layer and d_m, V_m, d_m/V_m, and $\mu V_m/d_m$, where $V_m\equiv\bar{u}_m(0)$ as the corresponding scales in the porous layer (the scales used are the as same as in Ref. [3]). In this study, we consider only two-dimensional perturbations and define the stream function ψ as $(\tilde{u},\tilde{w})=(\partial\psi/\partial z,-\partial\psi/\partial x)$, where the tilde indicates perturbations. We further apply normal-mode expansion of the form $\psi=\Phi(z)\exp(\sigma t+ikx)$, where Φ denotes the amplitude of the stream function, the real part of the complex eigenvalue σ

represents the time growth rate, and k is the streamwise wave number. Similarly, $\psi_m = \Phi_m(z_m)\exp(\sigma_m t_m + ik_m x_m)$. Note that $\sigma = \sigma_m \frac{\hat{d}^2 \mathrm{Re}_m}{\mathrm{Re}}$ and $k = k_m \hat{d}$, where the Reynolds numbers in the fluid and porous layers are given by $\mathrm{Re} = Vd/\nu$ and $\mathrm{Re}_m = V_m d_m/\nu$. Also note that $\mathrm{Re}_m = \frac{8\delta^2 \eta_x(0)}{F\hat{d}}\mathrm{Re}$.

Thus, letting $D = \frac{d}{dz}$ and $D_m = \frac{d}{dz_m}$, the linearized perturbation equations are given by

$$\frac{1}{\mathrm{Re}}(D^2-k^2)^2\Phi - ik\overline{U}(D^2-k^2)\Phi + ik\frac{d^2\overline{U}}{dz^2}\Phi = \sigma(D^2-k^2)\Phi, \tag{2.12}$$

$$\frac{1}{\delta^2}\left[\frac{D_m^2\Phi_m}{\eta_x} - \xi\frac{k_m^2\Phi_m}{\eta_z} - \frac{D_m\eta_x D_m\Phi_m}{\eta_x^2}\right] = \frac{-\mathrm{Re}_m\sigma_m}{\phi}\left(D_m^2 - k_m^2\right)\Phi_m, \tag{2.13}$$

subjected to the following boundary conditions.

At the base of the porous layer $z_m = -1$,

$$\Phi_m = 0. \tag{2.14}$$

At the interface $z = z_m = 0$,

$$\mathrm{Re}\Phi = \mathrm{Re}_m\Phi_m, \tag{2.15}$$

$$\frac{\mathrm{Re}}{\mathrm{Re}_m\hat{d}^3}\left[(D^2-k^2)D\Phi - \mathrm{Re}(ik\overline{U}+\sigma)D\Phi + ik\mathrm{Re}\frac{d\overline{U}}{dz}\Phi\right] = -\left[\frac{\mathrm{Re}_m\sigma_m}{\phi} + \frac{1}{\delta^2\eta_x(0)}\right]D_m\Phi_m, \tag{2.16}$$

$$D^2\Phi = \frac{\alpha_{BJ}\hat{d}}{\delta\sqrt{\eta_x(0)}}\left(D\Phi - \frac{\hat{d}\mathrm{Re}_m}{\mathrm{Re}}D_m\Phi_m\right). \tag{2.17}$$

At $z = 1$,

$$\Phi = D\Phi = 0. \tag{2.18}$$

III. RESULTS

Equations (2.12) and (2.13), along with the boundary conditions, are solved using the Chebyshev spectral collocation method (for details, see [4]). Unless otherwise stated, the parameters assume the nominal values $\delta = 0.001$, $A = 0$, $\xi = 1$, $\phi = 0.3$, and $\alpha_{BJ} = 0.1$. Wherever a comparison is possible, the neutral stability curves corresponding to the isotropic and homogeneous case presented in the figures (to be shown later) agree with those reported by Chang *et al.* [3], except for the multivaluedness, which as Liu *et al.* [4] point out was overlooked in that paper. This serves as a validation of our numerical code.

A. Effect of anisotropy

To examine the effect of anisotropy alone, we assume the permeability to be homogeneous, i.e., $\eta_x = \eta_z = 1$. Figure 1 shows the neutral stability curves for different values of the anisotropy parameter, ξ and δ for $\hat{d} = 0.1$. The critical Reynolds number, Re_c, along with the dominant mode for all the cases presented in this section is listed in Table I.

At $\delta = 0.002$ [Fig. 1(a)], the relatively high permeability allows the flow perturbations to permeate through the thick porous layer, thereby leading to the strong dominance of PM over other modes, irrespective of the value of ξ. However, a reduction in ξ is found to destabilize PM (neutral curves shift to lower Reynolds numbers). This is logically understood by observing that for a fixed $\hat{d}$ and δ, a reduction in ξ translates to an increase in permeability in the z direction and a subsequent reduction in the flow resistance, thus destabilizing the flow.

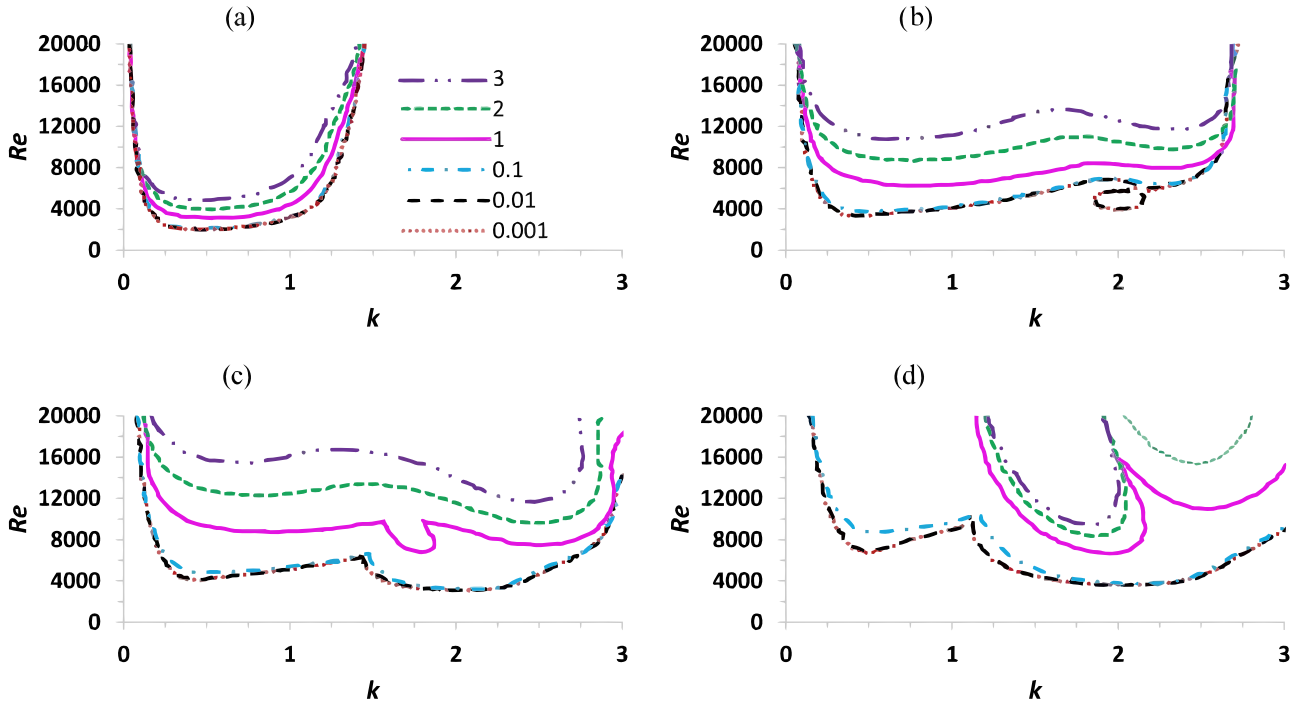

FIG. 1. (Color online) Neutral curves for different values of ξ (as given in the legend) with $\hat{d} = 0.1$ and (a) $\delta = 0.002$, (b) $\delta = 0.001$, (c) $\delta = 0.0008$, (d) $\delta = 0.0005$. Legends are the same in all the plots.

TABLE I. Variation of Re_c with the anisotropy parameter (ξ) for different values of depth ratio ($\hat{d}$) and Darcy number (δ). The most unstable mode in each case is indicated in brackets.

$\hat{d}$	ξ \ δ	0.002	0.001	0.0008	0.0005
0.1	0.001	2047 (PM)	3275 (PM)	3099 (EFM)	3626 (EFM)
	0.01	1988 (PM)	3333 (PM)	3099 (EFM)	3626 (EFM)
	0.1	2164 (PM)	3743 (PM)	3216 (EFM)	3743 (EFM)
	1	3099 (PM)	6261 (PM)	6764 (EFM)	6667 (EFM)
	2	3977 (PM)	8655 (PM)	9649 (OFM)	8363 (EFM)
	3	4795 (PM)	10760 (PM)	11637 (OFM)	9474 (EFM)
0.12	0.001		3041 (EFM)		
	0.01		3099 (EFM)		
	0.1		3216 (EFM)		
	0.4		4269 (EFM)		
	0.8		6667 (EFM)		
	1		7341 (OFM)		
	2		9474 (OFM)		
	3		11521 (OFM)		
0.13	0.001		3099 (EFM)		
	0.01		3041 (EFM)		
	0.1		3099 (EFM)		
	0.4		4152 (EFM)		
	0.8		5556 (EFM)		
	1		6297 (EFM)		
	2		9532 (EFM)		
	3		11988 (OFM)		
0.2	0.001	3450 (PM)	3626 (EFM)	4094 (EFM)	5497 (EFM)
	0.01	3509 (PM)	3567 (EFM)	4152 (EFM)	5322 (EFM)
	0.1	3918 (PM)	3743 (EFM)	4269 (EFM)	5789 (EFM)
	1	6327 (PM)	6667 (EFM)	7602 (EFM)	9854 (EFM)
	2	8713 (PM)	8363 (EFM)	9357 (EFM)	11462 (EFM)
	3	10760 (PM)	9532 (EFM)	10468 (EFM)	12398 (EFM)
0.3	0.001	3041 (EFM)	4211 (EFM)	4678 (EFM)	
	0.01	3099 (EFM)	4269 (EFM)	4678 (EFM)	
	0.1	3275 (EFM)	4737 (EFM)	5556 (EFM)	
	1	5965 (EFM)	8585 (EFM)	9591 (EFM)	
	2	7895 (EFM)	10292 (EFM)	11228 (EFM)	
	3	9123 (EFM)	11287 (EFM)	12222 (EFM)	

Re_c is more sensitive to an increase in ξ than it is to a decrease in ξ. Further, the effect of decrease in ξ is weakened for $\xi > 0.1$ where the marginal curves almost coincide. At $\delta = 0.001$ [Fig. 1(b)], due to the reduction in permeability, OFM also becomes significant leading to bimodal neutral stability curves. As with the case of $\delta = 0.002$, the dominant mode continues to be PM regardless of the value of ξ and the destabilization effect of a decrease in ξ is also observed for the reasons already stated. Also, note the higher sensitivity of Re_c to an increase in ξ; a mere doubling of ξ from 1 to 2 has resulted in an almost twofold increase in Re_c, whereas to effect a twofold decrease in Re_c, an order of magnitude reduction in ξ is required. Here, however, we also observe the appearance of a looplike mode in the medium-wave range when $\xi < 0.1$ [Fig. 1(b)]. This new mode is found to occur at extremely low values of ξ in cases where bimodal instability (constituted by PM and OFM) prevails [see also Fig. 2(a)]. But, even in these rare cases where it appears, this mode never dominates the system stability. Hence, we do not wish to address this mode in detail, except to point out that though it appears in the medium-wave region, it has no connection with EFM. EFM indeed exists in those cases in the very high Re region and is completely dominated by the bimodal instability (hence not shown in the graphs).

At $\delta = 0.0008$ [Fig. 1(c)] for the isotropic case ($\xi = 1$; the solid curve), the neutral curve is trimodal, with EFM now being the most unstable mode. For other values of ξ, the neutral curves are observed to be bimodal in nature. As expected, the general destabilizing trend due to a decrease in ξ is seen; however, unlike the previous two cases, a shift in dominance between the two fluid modes also occurs with a change in ξ. A lower ξ favors EFM, but a higher ξ favors OFM (also see Table I). Since both of these modes are shear generated [3], it is to be understood that the variation of K_z affect the shear stress distribution in a rather complicated way. The consequence is that a change in ξ has different degrees of influence on the two modes; at lower ξ, the destabilization effect is greater for EFM causing its dominance over OFM and at higher ξ, the stabilization effect is lesser for OFM causing its dominance over EFM. At even lower permeability

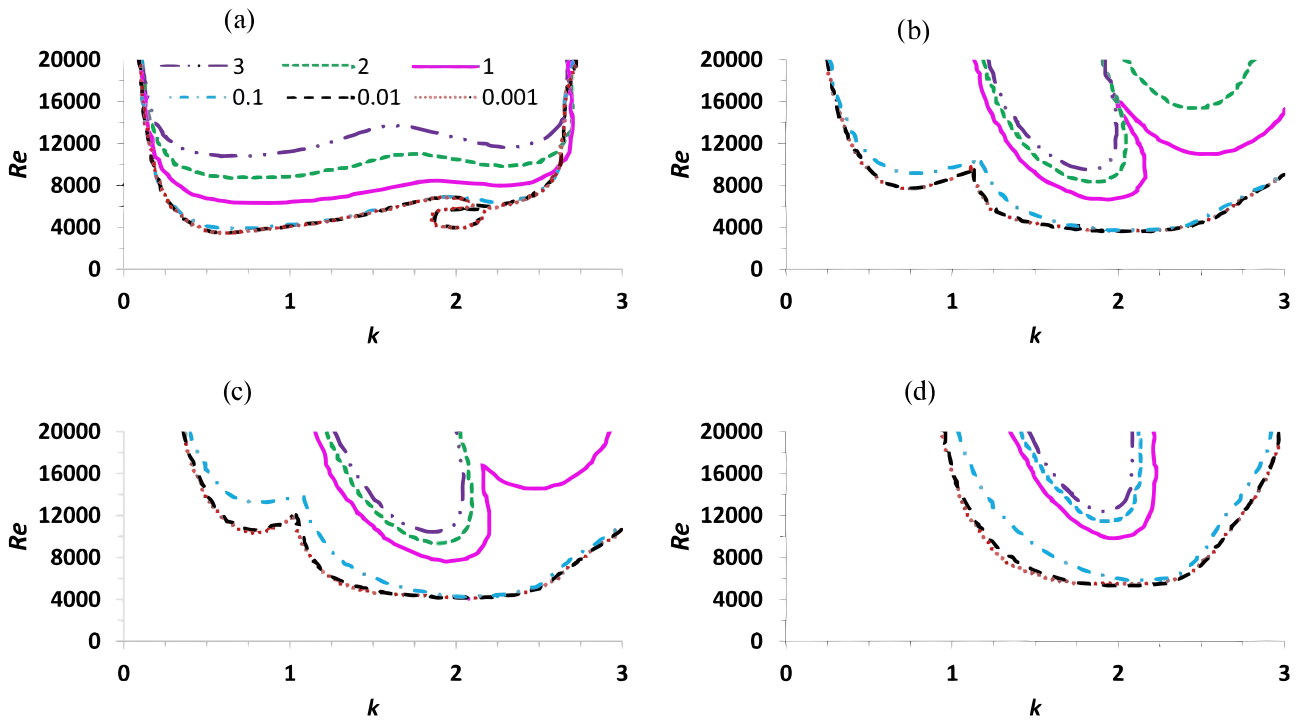

FIG. 2. (Color online) Neutral curves for different values of ξ with $\hat{d} = 0.2$ and (a) $\delta = 0.002$, (b) $\delta = 0.001$, (c) $\delta = 0.0008$, (d) $\delta = 0.0005$. Legends are the same in all the plots.

of $\delta = 0.0005$ [Fig. 1(d)], EFM is always the most unstable mode (with the expected destabilizing effect of a decrease in ξ). Note that mode switching is absent in this case. Along with the data to be presented subsequently for higher depth ratios, this indicates that the switching of mode dominance with change in ξ is observed only for low values of $\hat{d}$ and intermediate values of δ. In other words, switching of mode dominance appears to occur as a result of anisotropic variations in permeability, only under conditions (set by other system parameters) that are borderline between regions where OFM and EFM are most likely to dominate.

Figure 2 presents the marginal curves for the same conditions as in Fig. 1, but at a higher depth ratio of $\hat{d} = 0.2$. In all cases, the general trend of the destabilizing effect of decrease in ξ may be noted. At $\delta = 0.002$ [Fig. 2(a)], as opposed to the corresponding case with lower depth ratio [Fig. 1(a), where the only mode present is PM], due to a relatively thicker fluid layer, the neutral curves are bimodal with the additional presence of OFM; nonetheless PM is the dominant mode of instability. Additionally, Re_c is higher for a particular ξ (also refer Table I); i.e., PM becomes more stable with an increase in the depth ratio. A similar observation was also made by Liu *et al.* [4] with Brinkman's model for the low-porosity case. At a lower permeability of $\delta = 0.001$ [Fig. 2(b)], EFM becomes the dominant mode with PM appearing in the low-wave-number space for lower ξ (or higher relative permeability in the z direction) and OFM appearing in the high-wave-number region for higher ξ (or lower relative permeability in the z direction). The neutral curves at $\delta = 0.0008$ [Fig. 2(c)] also follow qualitatively similar trends but quantitatively they are shifted slightly upwards. The stabilizing effect, as already stated, can be attributed to the higher resistance offered by a less-permeable porous layer. At $\delta = 0.0005$ [Fig. 2(d)], the system is completely dominated by EFM. Comparison with the corresponding curves at a higher permeability of $\delta = 0.0008$ [Fig. 2(c)] suggests that the stabilizing effect due to the reduction in permeability is more pronounced at higher values of ξ. Also note that in Fig. 2(d), Re_c increases by more than a factor of 2 within the range of ξ considered. This shows that even though EFM is a pure fluid mode, it is significantly affected by the anisotropic change in the permeability of the porous medium.

At $\hat{d} = 0.3$ (see Fig. 3), flow instability is completely contained in the thick fluid layer. As a result EFM is the most unstable mode regardless of the values of δ and ξ. Figure 3 also shows that a lower ξ or a higher δ destabilizes the system; trends that are consistent with the above reasoning. A comparison with the results for $\hat{d} = 0.2$ reveals that, similar to PM, EFM also becomes more stable with a higher depth ratio (see also Table I), possibly due to less shear intensity in the flow due to a thicker fluid layer. Before moving on to the inhomogeneity effects, in Fig. 4 we present the marginal stability curves for two important depth ratios, namely, $\hat{d} = 0.12$ [where OFM dominates the system in the nominal (isotropic) case] and 0.13 (the threshold that marks the shift in dominance between the porous mode and fluid mode in the thermal convection problem in a superposed fluid-porous system) at the nominal value of $\delta = 0.001$. Note that two additional curves are plotted, corresponding to $\xi = 0.4$ and 0.8, to reveal the transition better. As already explained, in both these cases, OFM and EFM compete with each other for dominance with change in ξ similar to Fig. 1(c). For a smaller ξ, EFM is more unstable, whereas for a larger ξ, OFM is more critical.

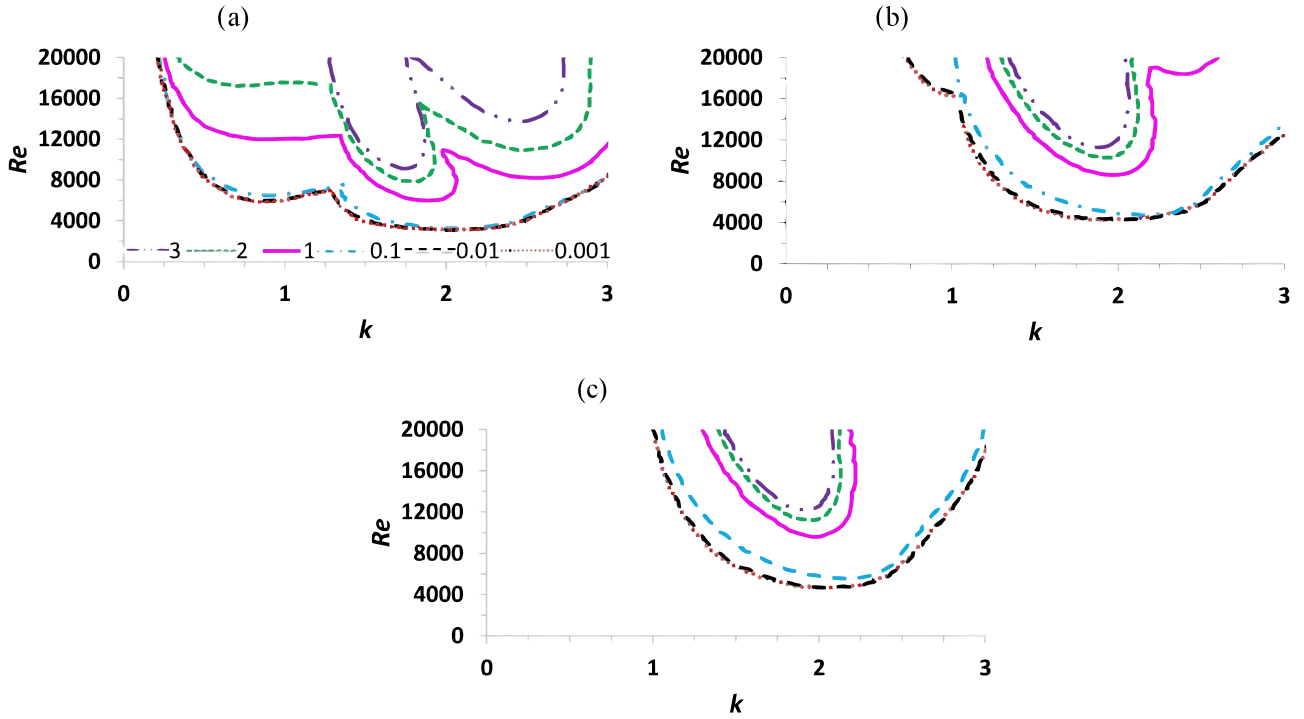

FIG. 3. (Color online) Neutral curves for different values of ξ with $\hat{d} = 0.3$ and (a) $\delta = 0.002$, (b) $\delta = 0.001$, (c) $\delta = 0.0008$. Legends are the same in all the plots.

B. Effect of inhomogeneity

Here we exclude the anisotropic effects by setting $\xi = 1$ and using the same homogeneous variations of permeability [15] in the principal directions, namely, $\eta_x = \eta_z = e^{A(1+z_m)}$. At the bottom ($z_m = -1$), $\eta_x = \eta_z = 1$ and the permeabilities in the x and z directions increase (decrease, respectively) vertically with a positive (negative, respectively) value of A. Green and Freehill [16] used linear inhomogeneity functions, but we choose to use the exponential inhomogeneity functions as they model a practical scenario [15]. Moreover, since our aim here is to illustrate the effect of inhomogeneity per se, we do not attach much importance to the actual functional forms of η_x and η_z. By retaining the same exponential form for these functions, we change the value of the parameter A to understand the effect of the degree of inhomogeneity on the system stability.

From the discussion that follows, it may appear that the effect of changing the parameter A is equivalent to that of changing the average permeability of the porous medium. But one should keep in mind that its effects are far more dramatic in that the velocity profile in the porous medium as well as that in the fluid layer (through the interfacial slip velocity) are affected by a change in the parameter A [see Eqs. (2.8) and (2.9)]. The inhomogeneous modulation of permeability

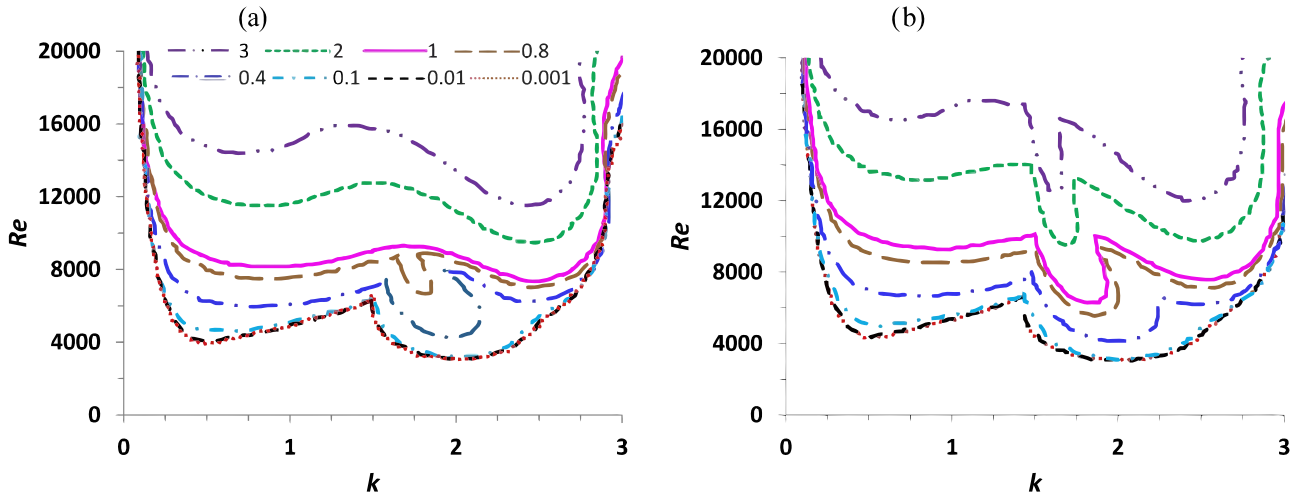

FIG. 4. (Color online) Neutral curves for different values of ξ with $\delta = 0.001$ and (a) $\hat{d} = 0.12$, (b) $\hat{d} = 0.13$. Legends are the same in both the plots.

allows more control on the stability dynamics of the system than a variation in the mean permeability. The latter effect is incidentally captured by the variation in the Darcy number as discussed in the previous section or in Chang *et al.* [3]. In this section, the sole effect of varying degrees of homogeneity along the depth of the porous layer is addressed.

One would anticipate the effects of inhomogeneity to be less predictable than that of anisotropy, because the inhomogeneity functions appear in the perturbation equations in a more complex way [see Eq. (2.13)]. In our previous paper [10], we have shown that the effect of inhomogeneous permeability on instability characteristics of a similar two-layer system is indeed rather complicated and (as will be shown by the data presented subsequently) this is true in the present problem as well. In contrast to the effects of anisotropic variations of permeability, the following features are commonly observed with inhomogeneity variation for a given case: a change in the range of unstable wave numbers and switching of mode dominance which results in a subsequent nonmonotonic trend of global minimum of the marginal curve, Re_c. Even so, a pattern that is consistent with physical expectations can be recognized in the trend of Re_c corresponding to a particular mode. As A increases, Re_c of a given mode is observed to decrease monotonically in nearly all the cases considered, a behavior attributable to the lower flow resistance offered by the porous medium. The progression pattern of the most dominant mode itself is consistent with the physical picture discussed in Sec. III A and Chang *et al.* [3]. A parametric change that leads to a very high net permeability of the porous layer causes PM to be the dominant instability. On the other extreme, for very low overall permeability, EFM becomes the most unstable mode as the effect of the porous layer is insignificant. Under intermediate conditions, where the effect of the porous layer is strong enough, OFM is the most critical mode of instability.

Marginal curves for different values of A and δ for $\hat{d} = 0.1$ are shown in Fig. 5. At $\delta = 0.002$ for the homogeneous case (solid curve), PM is the dominant mode. As A is decreased to –1 (a vertically decreasing permeability), PM becomes more stable (also see Table II) in terms of Re_c, which can be explained based on the increased flow resistance. We notice, however, that the area of unstable zone expands out to the higher-wave-number region, i.e., lower-wavelength disturbances become relatively more unstable compared to the homogeneous case. As mentioned earlier, such a change in the range of unstable wave numbers is not observed in PM as a result of anisotropic variations [e.g., cf. Fig. 1(a)], again emphasizing the drastic influence of inhomogeneous variations. At $A = -2$, the net permeability of the porous medium is so low that all the instability is now confined to the fluid layer, leading to the dominance of EFM. On the other hand, at $A = 1$, due to the increase in the net permeability, we observe a slight destabilization of PM compared to the homogeneous case in terms of Re_c, but the mode shrinks in the k-Re plane.

At $A = 2$, both Re_c and the area of unstable zone show a stabilizing effect. The mode becomes very narrow in the k-Re plane. In the parameter space considered, this is the only case where Re_c of a given mode (PM in this case) shows a stabilizing effect with increase in A, which thus far cannot be explained in simple physical terms. But we reemphasize that given the complexity of the problem, occurrence of such counterintuitive behavior is plausible, if not inevitable. Figure 5(a) illustrates that as far as PM is concerned, increasing A has the effect of filtering out short-wave flow perturbations. It is physically acceptable that a more-permeable porous layer

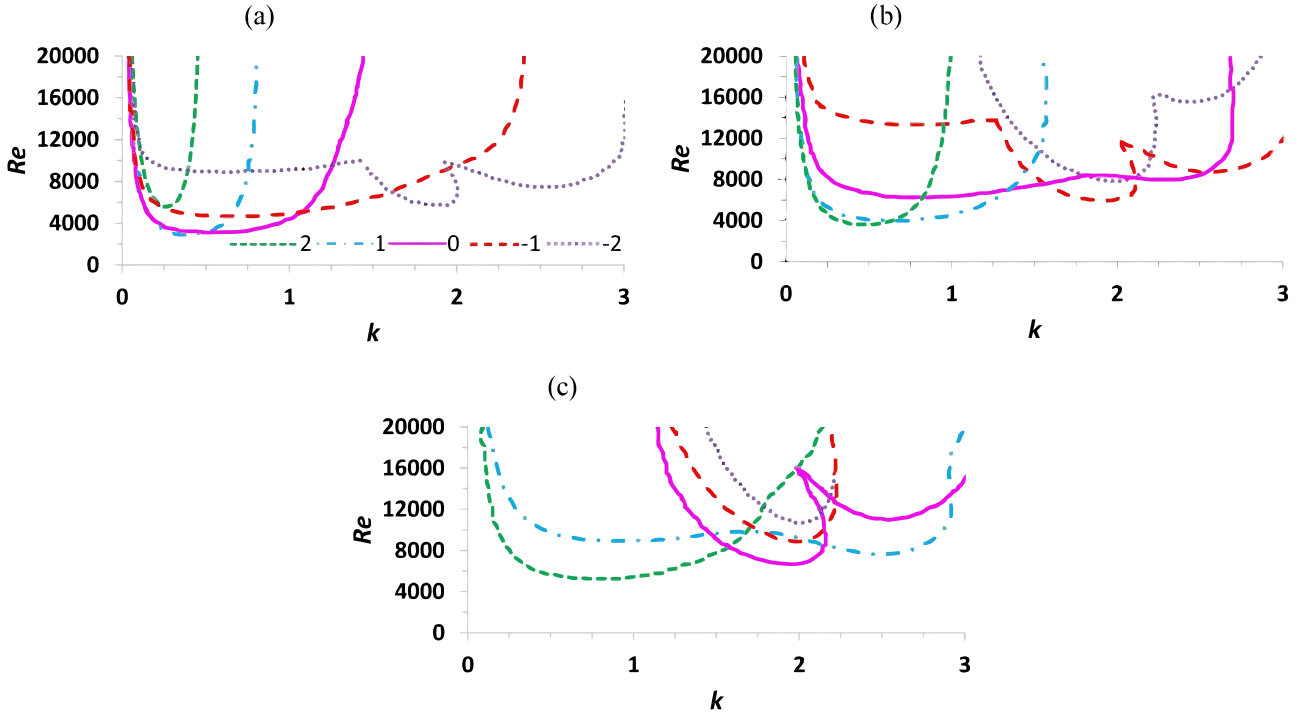

FIG. 5. (Color online) Neutral curves for different values of A with $\hat{d} = 0.1$ and (a) $\delta = 0.002$, (b) $\delta = 0.001$, (c) $\delta = 0.0005$.

TABLE II. Variation of Re_c with the inhomogeneity factor (A) for different values of depth ratio ($\hat{d}$) and Darcy number (δ). The most unstable mode in each case is indicated in brackets.

$\hat{d}$	A \ δ	0.002	0.001	0.0005
0.1	–2	5731 (EFM)	7836 (EFM)	10700 (EFM)
	–1	4678 (PM)	5965 (EFM)	8889 (EFM)
	0	3100 (PM)	6261 (PM)	6670 (EFM)
	1	2866 (PM)	3977 (PM)	7661 (OFM)
	2	5570 (PM)	3626 (PM)	5263 (PM)
0.12	–2		8713 (EFM)	
	–1		6491 (EFM)	
	0		7340 (OFM)	
	1		4678 (PM)	
	2		3860 (PM)	
0.13	–2		9064 (EFM)	
	–1		6784 (EFM)	
	0		6297 (EFM)	
	1		5175 (PM)	
	2		3977 (PM)	
0.2	–2	7544(EFM)	10760 (EFM)	>20000
	–1	5848 (EFM)	8830 (EFM)	14152 (EFM)
	0	6330 (PM)	6670 (EFM)	9850 (EFM)
	1	4187 (PM)	7778 (OFM)	7778 (EFM)
	2	4269 (PM)	5789 (PM)	6667 (EFM)

will favor the evolution of high-wavelength disturbances. At $\delta = 0.001$ [Fig. 5(b)], all the modes are more stable due to the lower Darcy number. For the same reason, at $A = -2$, EFM almost completely suppresses all the other modes, whereas the neutral curve for the same value of A at $\delta = 0.002$ is trimodal [Fig. 5(a)]. Note that Re_c of a given mode does exhibit a monotonic increase with decrease in A. At $\delta = 0.0005$, a competition among all three modes can be observed. At $A = 1$, OFM is dominant; higher A favors PM and lower A favors EFM. As seen in the previous case, the local minimum corresponding to a given mode shows the stabilizing (destabilizing) effect with a decreasing (an increasing) A.

Figure 6 shows the inhomogeneity effects at a higher $\hat{d}$ of 0.2. Compared to Fig. 5, the stabilization effect of a higher depth ratio is observed (for a quantitative comparison, refer to Table II), as was seen in the anisotropy case. The qualitative behavior of the results follows the expected pattern. Interestingly, the graph shown in Fig. 6(a) resembles that in Fig. 5(b) quantitatively as well as qualitatively. This means that for a given A, the stabilizing effect of doubling the depth ratio and the destabilizing effect of doubling the Darcy number almost cancel each other. The same holds for Figs. 6(b) and 5(c) (also see Table II). It is to be mentioned that a similar pattern can be observed in the results of anisotropic effect presented in Sec. III A. At $\delta = 0.0005$ [Fig. 6(c)], the flow stability is completely dominated by EFM and for $A = -2$, the flow is so stable that the marginal curve goes out of the range of Re considered here. Finally, for completeness, we present the neutral curves for $\hat{d} = 0.12$ and 0.13 in Fig. 7. At $\hat{d} = 0.12$, for the homogeneous case, OFM is dominant, a negative A causes EFM to dominate, and a positive A causes PM to dominate. At $\hat{d} = 0.13$, for the homogeneous and negative A cases, EFM is dominant, otherwise PM prevails.

IV. CONCLUDING REMARKS

Linear stability of Poiseuille flow in a fluid-porous system with anisotropic and inhomogeneous permeability has been analyzed. In the range of parameters considered, both

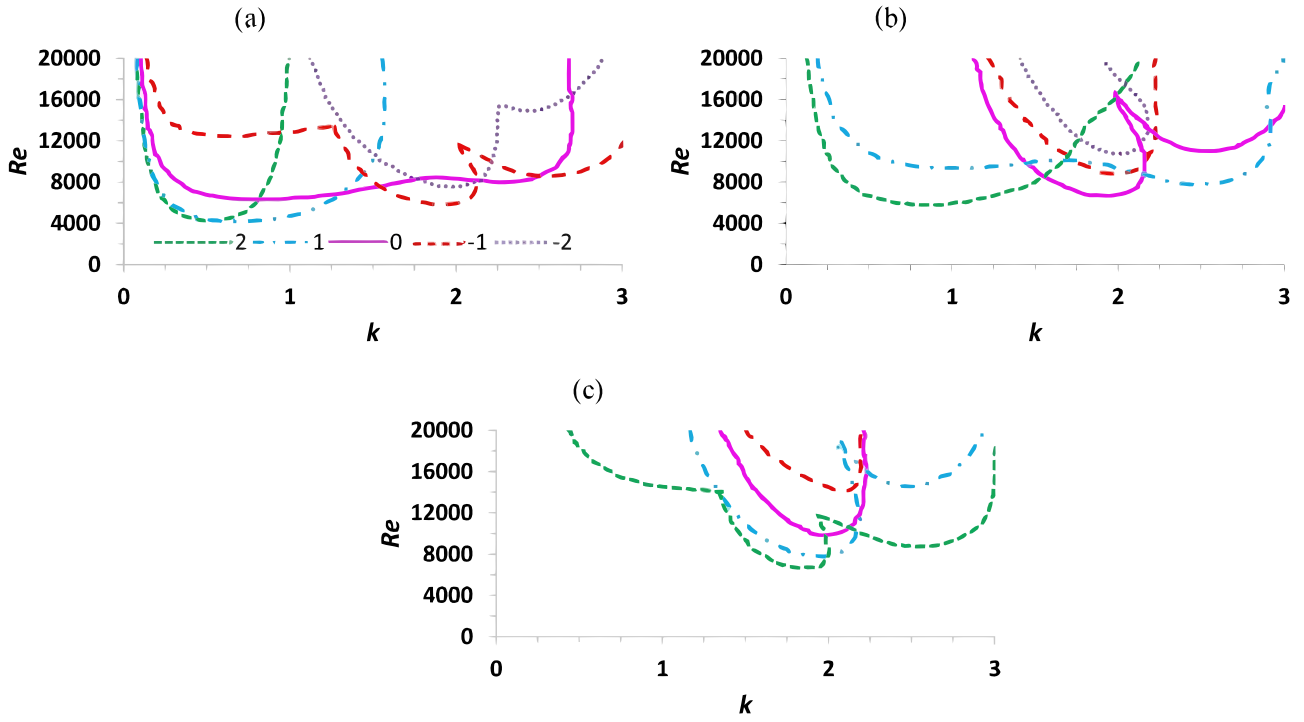

FIG. 6. (Color online) Neutral curves for different values of A with $\hat{d} = 0.2$ and (a) $\delta = 0.002$, (b) $\delta = 0.001$, (c) $\delta = 0.0005$.

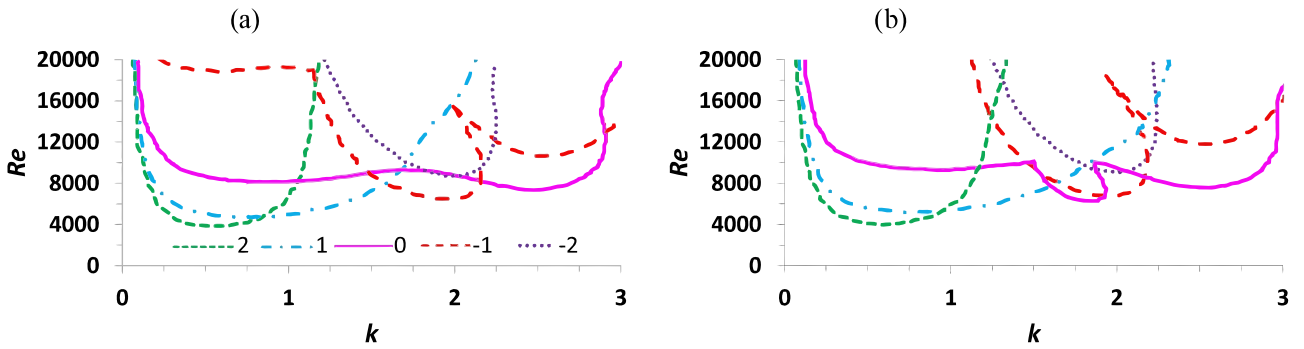

FIG. 7. (Color online) Neutral curves for different values of A with $\delta = 0.001$ and (a) $\hat{d} = 0.12$, (b) $\hat{d} = 0.13$. Legends are the same in all the plots.

directional and spatial variations in permeability are found to have an immense effect on the stability characteristics for all depth ratios and Darcy numbers. For example, referring to the nominal case [cf. Fig. 1(b)], doubling the permeability of the porous medium in the basic flow direction relative to that in the cross-stream direction (quantitatively expressed by the parameter ξ) increases Re_c by 38%. On the other hand, a reduction in ξ destabilizes the flow, albeit the effect is lesser compared to that of an increase in ξ. It is conceivable that the former finding can be exploited in applications where instability is not desirable (e.g., manufacture of composite materials). On the other hand, in applications where the instability is a desired phenomenon (e.g., packed-bed heat exchangers), the latter information can be used; however, our results show that the destabilizing effect plateaus out below $\xi = 0.1$. Likewise, an inhomogeneous variation that increases the overall permeability of the porous medium has destabilizing effects on the modes.

In addressing the question of which instability mode is most unstable when the permeability is allowed to be anisotropic or inhomogeneous, one sees a striking difference between the two effects: while switching of mode dominance is observed only under rare transitional conditions for anisotropic variations in permeability, it is a common result for inhomogeneous variations. In addition, competition for dominance is observed only between the fluid modes as a result of anisotropic effects, a case in point being at low depth ratio and intermediate permeability [Fig. 1(c)]. A lower ξ is found to favor the dominance of EFM and a higher ξ favors OFM. As for the inhomogeneous effects, a low (negative) value of A is found to favor EFM, a high (positive) value favors PM, and intermediate values favor OFM. These qualitative trends are all physically consistent. The drastic influence of inhomogeneous effects is also evident in the fact that for a given mode, the range of unstable wave numbers changes considerably with A. Further, only local minima of the neutral curves (or the critical Reynolds number of a particular mode) are observed to exhibit a monotonic response with A. On the other hand, in the case of anisotropic variations, the global minimum (Re_c) of the curves itself displays a monotonic behavior.

To summarize the main outcomes of the present work, the following are the factors that stabilize the system:

(a) decrease in Darcy number (or loosely, the permeability of the porous medium),
(b) increase in depth ratio,
(c) increase in the anisotropy parameter ξ, and
(d) decrease in the inhomogeneity factor, A.

ACKNOWLEDGMENTS

S.B. acknowledges the Solar Energy Research Institute in India and the United States (SERIIUS) for financial support.

[1] D. A. Nield and A. Bejan, *Convection in Porous Media* (Springer Science & Business Media, Berlin, 2006).
[2] F. Chen and C. F. Chen, Onset of finger convection in a horizontal porous layer underlying a fluid layer, J. Heat Transfer **110**, 403 (1988).
[3] M.-H. Chang, F. Chen, and B. Straughan, Instability of Poiseuille flow in a fluid overlying a porous layer, J. Fluid Mech. **564**, 287 (2006).
[4] R. Liu, Q. S. Liu, and S. C. Zhao, Instability of plane Poiseuille flow in a fluid-porous system, Phys. Fluids **20**, 104105 (2008).
[5] A. A. Hill and B. Straughan, Poiseuille flow in a fluid overlying a porous medium, J. Fluid Mech. **603**, 137 (2008).
[6] N. Silin, J. Converti, D. Dalponte, and A. Clausse, Flow instabilities between two parallel planes semi-obstructed by an easily penetrable porous medium, J. Fluid Mech. **689**, 417 (2011).
[7] B. Straughan and D. W. Walker, Anisotropic porous penetrative convection, Proc. R. Soc. London, Ser. A **452**, 97 (1996).
[8] M. Badiey, H.-D. A. Cheng, and J. Indra, Deterministic and stochastic analyses of acoustic plane-wave reflection from inhomogeneous porous seafloor, J. Acoust. Soc. Am. **99**, 903 (1996).
[9] M. S. Malashetty and S. Mahantesh, The onset of convection in a binary fluid saturated anisotropic porous layer, Int J. Therm. Sci **49**, 867 (2010).
[10] P. Deepu, S. Dawande, and S. Basu, Instabilities in a fluid overlying an inclined anisotropic and inhomogeneous porous layer, J. Fluid Mech. **762**, R2 (2015).

[11] R. Liu and Q. Lu, Instabilities of a liquid film flowing down an inclined porous plane, Phys. Rev. E **80**, 036316 (2009).

[12] H. N. Kandel and J. P. Pascal, Inclined fluid-film flow with bottom filtration, Phys. Rev. E **88**, 052405 (2013).

[13] J. M. Floryan, S. H. Davis, and R. E. Kelly, Instabilities of a liquid film flowing down a slightly inclined plane, Phys. Fluids **30**, 983 (1987).

[14] G. S. Beavers and D. D. Joseph, Boundary conditions at a naturally permeable wall, J. Fluid Mech. **30**, 197 (1967).

[15] F. Chen, Salt-finger instability in an anisotropic and inhomogeneous porous substrate underlying a fluid layer, J. Appl. Phys. **71**, 5222 (1992).

[16] T. Green and R. L. Freehill, Marginal stability in inhomogeneous porous media, J. Appl. Phys. **40**, 1759 (1969).